LETTERS
https://doi.org/10.1038/s41563-019-0473-6

nature materials

A window to trap-free charge transport in organic semiconducting thin films

Naresh B. Kotadiya, Anirban Mondal, Paul W. M. Blom, Denis Andrienko and Gert-Jan A. H. Wetzelaer*

Organic semiconductors, which serve as the active component in devices, such as solar cells, light-emitting diodes and field-effect transistors[1], often exhibit highly unipolar charge transport, meaning that they predominantly conduct either electrons or holes. Here, we identify an energy window inside which organic semiconductors do not experience charge trapping for device-relevant thicknesses in the range of 100 to 300 nm, leading to trap-free charge transport of both carriers. When the ionization energy of a material surpasses 6 eV, hole trapping will limit the hole transport, whereas an electron affinity lower than 3.6 eV will give rise to trap-limited electron transport. When both energy levels are within this window, trap-free bipolar charge transport occurs. Based on simulations, water clusters are proposed to be the source of hole trapping. Organic semiconductors with energy levels situated within this energy window may lead to optoelectronic devices with enhanced performance. However, for blue-emitting light-emitting diodes, which require an energy gap of 3 eV, removing or disabling charge traps will remain a challenge.

Theories of charge transport in organic semiconductors predict that for most materials the charge-carrier mobility should be similar for electrons and holes[1]. In experiments, however, the transport of one type of carrier is usually clearly superior. In field-effect transistor geometries, this has been ascribed to the limited injection capabilities of commonly used electrodes[2] and charge trapping at the semiconductor/dielectric interface[3]. However, there seems to be a more fundamental factor causing unipolarity in the bulk transport of organic semiconductors, not related to interfaces at the electrodes or gate insulator. For example, bulk hole transport is dominant in most solution-processed conjugated polymers, being orders of magnitude higher than electron transport. By systematically varying the electron affinity of these polymers, it was found that electron trapping in the bulk is the reason for the low electron mobilities[4]. The trap depth reduces with increasing electron affinity (EA), suggesting the presence of a general impurity acting as the electron trap, with an EA of around 3.6 eV. For this reason, polymers with EAs higher than 3.6 eV can exhibit trap-free electron transport, which is a design rule for the realization of n-type conducting polymers[4].

Here, we first generalize this concept of electron trapping for organic semiconductors by including measurements on vacuum-deposited small-molecular semiconductors. We then demonstrate that not only electron transport becomes trap limited when the EA is below 3.6 eV, but also that hole transport will be hindered by trapping when the ionization energy (IE) of the material exceeds 6 eV, implying that trap-free charge transport is only observed within this energy window.

Hole transport in materials with IEs above 6 eV could previously not be measured, due to a lack of electrode materials with a sufficiently high work function to form an Ohmic hole contact. When measuring the hole current through an organic semiconductor in a hole-only device structure, it is essential that the injecting electrode does not exhibit an injection barrier. Otherwise, the measured current will be predominantly controlled by the injection rate, rather than the charge transport inside the organic semiconductor. Recently, we have developed a technique to create Ohmic hole contacts on organic semiconductors with IEs beyond 6 eV (ref. [5]).

Using this technique, we have here characterized the hole and electron transport for a large variety of organic semiconductors, both polymers and small molecules, by measuring the current density (J)–voltage (V) characteristics of hole- and electron-only devices. In the case of trap-free charge transport, the current depends on the square of the voltage, according to the Mott-Gurney square law for space-charge-limited currents[6]. However, when charge transport is trap limited, the current exhibits stronger voltage dependence, according to a power law $J \propto V^m$ with $m > 2$ (ref. [7]). The slope m of the J–V characteristics on a double-logarithmic scale can therefore be used as a fingerprint of trap-limited transport.

Figure 1 shows the slope (m) of the current density-voltage characteristics of single-carrier devices plotted versus the IE or EA of the investigated materials. For electron transport, as observed for both conjugated polymers and small molecules, a slope higher than two is measured when the EA of the organic semiconductor is lower than ~3.6 eV, indicating trap-limited electron transport with this regime. Remarkably, for IEs higher than 6 eV, hole transport also becomes trap limited. Consequently, for both electrons and holes, trap-free charge transport ($m = 2$) is measured when the EA (electron transport) or IE (hole transport) lies between 3.6 and 6.0 eV. As such, we have identified an energy window for trap-free charge transport in organic semiconductors spanning approximately 2.4 eV.

The absence of trapping for materials inside the trap-free window has been confirmed with thickness-dependent measurements[5,8–15], typically covering a thickness range of 100 to 300 nm, and transient transport measurements further supported the obtained steady-state mobilities[14,16] (see also Supplementary Fig. 12). In most cases, the trap-limited currents were observed even for relatively thin layers of close to 100 nm, in which the charge-carrier density is comparatively high. When Ohmic contacts are applied, charge carriers will diffuse from the contact into the semiconductor to establish thermodynamic equilibrium across the interface. The thinner the semiconductor film, the more diffused carriers will fill the traps. Since trap-limited currents are observed even for thin layers, trapping is severe and important for device-relevant layer thicknesses. Consequently, a trap-filled limit, in which all traps are filled

Max Planck Institute for Polymer Research, Mainz, Germany. *e-mail: wetzelaer@mpip-mainz.mpg.de

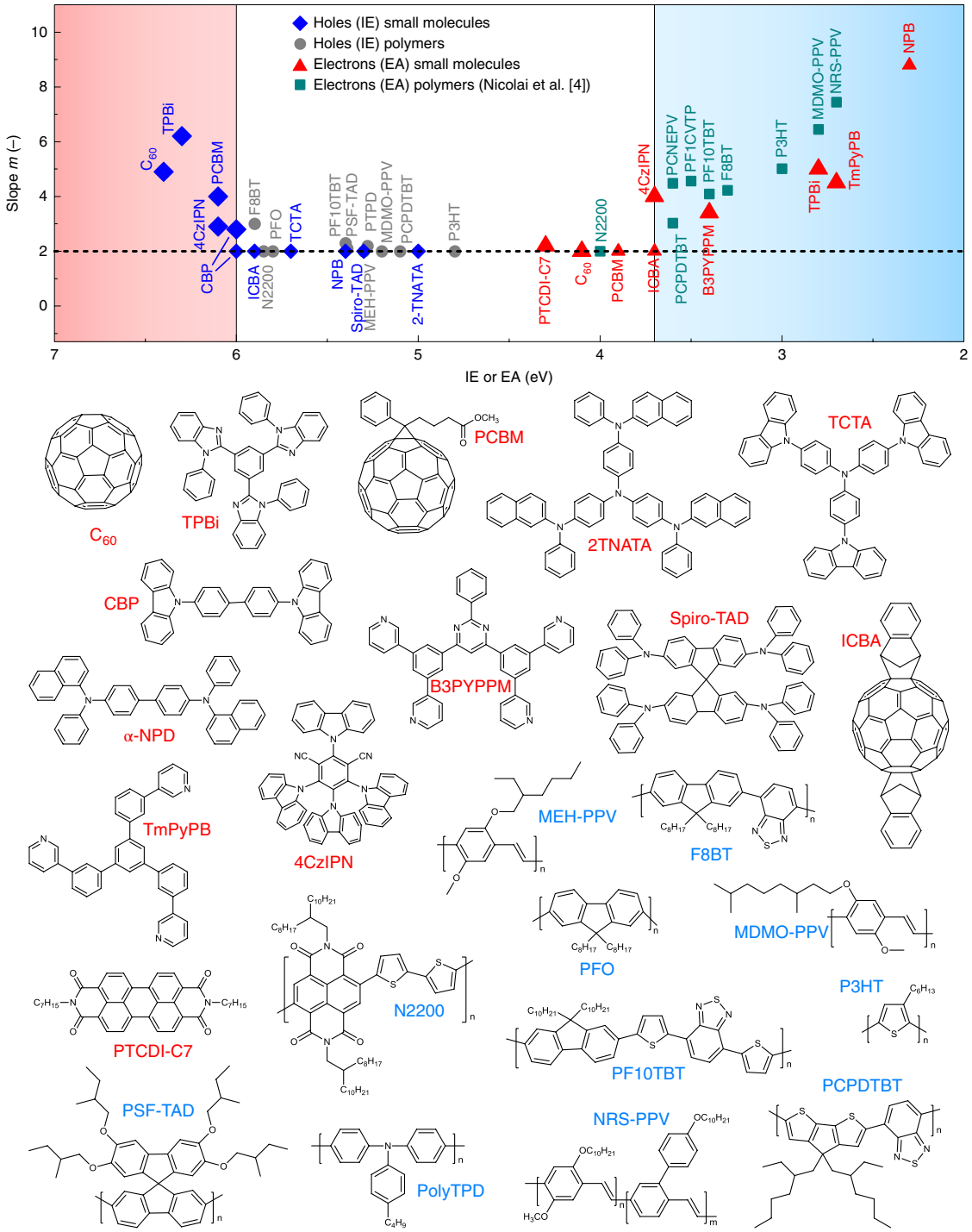

Fig. 1 | Energy window for trap-free charge transport. The top panel displays the slope of the hole or electron current versus IE or EA of the organic semiconductor, respectively. The symbols are divided into groups representing either electron or hole transport in either small molecules or polymers. Larger symbols represent data measured in this study (see Supplementary Figs. 1–11); small symbols are slopes determined from *J*–*V* characteristics from literature[4,5,8–13,26]. The dashed line marks a slope of two, characteristic of a trap-free space-charge-limited current. Trap-limited currents ($m > 2$) for electrons and holes are marked by the blue and red shaded areas, respectively. The chemical structures of the investigated molecules are displayed in the bottom panel and listed in Supplementary Table 1.

by injected charge carriers, was generally not observed, except for PCBM and CBP as discussed in detail below.

An interesting class of materials to exemplify the onset of universal hole trapping are fullerenes, which are commonly known for their good electron-transport properties. As shown in Fig. 2, for the fullerene derivatives C_{60} and PCBM with IEs of 6.4 and 6.1 eV, respectively, the current has a strong voltage dependence, with slopes of 4.9 and 4.0, respectively, indicating trap-limited hole transport. By contrast, the fullerene derivative ICBA, with a lower IE of 5.9 eV, exhibits a high hole current that depends quadratically on voltage, indicative of trap-free charge transport. Therefore, the presence or absence of hole trapping in these fullerene derivatives

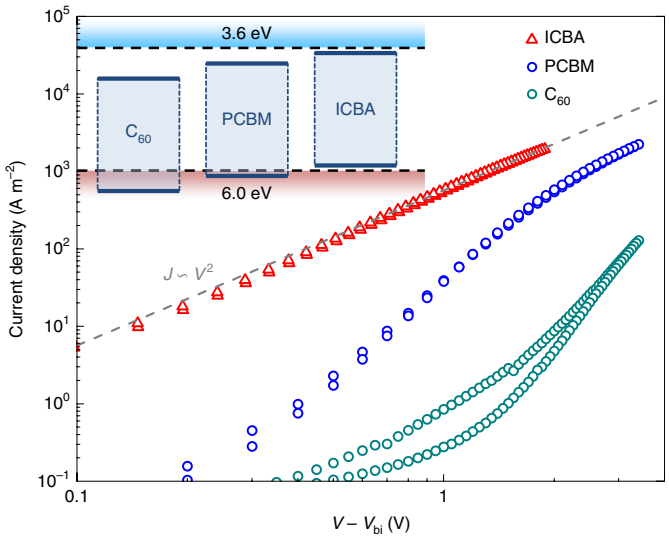

Fig. 2 | Hole transport in C_{60}, PCBM and ICBA. Current density versus voltage characteristics of ICBA (213 nm), PCBM (222 nm) and C_{60} (227 nm) hole-only devices, corrected for the built-in voltage (V_{bi}). The grey dashed line indicates a quadratic voltage dependence ($m=2$). The inset shows a schematic energy diagram, indicating the IE and EA (solid lines) of the fullerene derivatives with respect to the trap-free window (horizontal

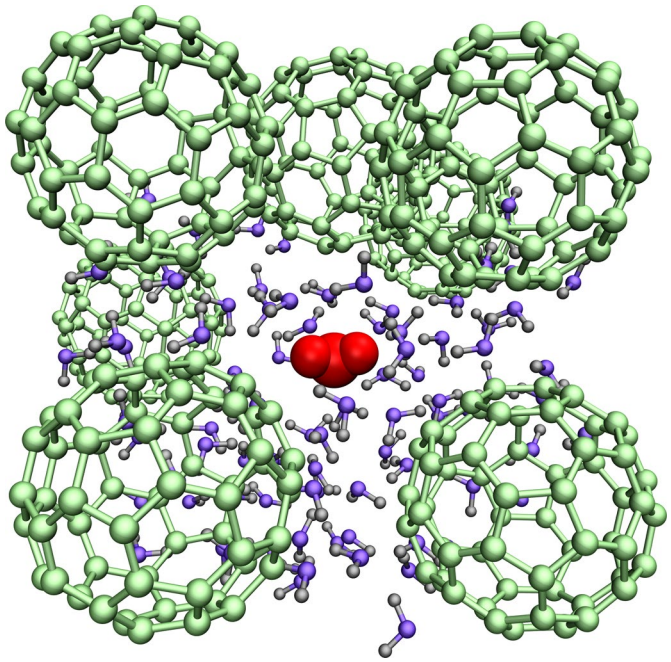

Fig. 3 | Close-up view of a water-filled pocket in a simulated C_{60} morphology. Molecular-dynamics simulation of the morphology of C_{60} (green) with water molecules (oxygen violet, hydrogen grey) filling the intermolecular voids. The red water molecule surrounded by a water shell has an IE of approximately 6 eV and is therefore a hole trap in C_{60}.

is directly related to their IE with respect to the trap-free window. Since the EA of ICBA, 3.7 eV, is also situated in this energy window, electron and hole transport are both trap free and nearly balanced[8]. Similarly, trap-free transport for both electrons and holes has been observed in the polymer N2200 and a diketopyrrolopyrrole-based polymer, which also fall within the trap-free window[9,17].

The ICBA hole mobility of $1.4\times10^{-3}\,cm^2\,V^{-1}\,s^{-1}$ extracted from space-charge-limited currents is very similar to the electron mobility[8], as expected theoretically for organic semiconductors. For PCBM, the hole transport can also be described with a high hole mobility similar to the electron mobility, but with the addition of a hole-trap concentration of $10^{16}\,cm^{-3}$ (Supplementary Fig. 1). At high voltages, a transition to a less steep slope of the J–V characteristics are observed (Fig. 2), which indicates that the current approaches the trap-filled limit, reaching a hole mobility of approximately $10^{-3}\,cm^2V^{-1}\,s^{-1}$. The high hole mobility in PCBM is confirmed for a thin (75 nm) hole-only device, in which the higher charge density fills most of the traps, leading to almost trap-free hole transport. This shows that the intrinsic hole mobility of PCBM is not low, but that the hole transport is hindered by—possibly extrinsic—hole traps.

From these results, it is clear that hole and electron transport in organic semiconductors becomes trap-limited for IEs larger than 6.0 eV and EAs smaller than 3.6 eV, respectively. For electron transport, molecular oxygen[18,19] and water-oxygen complexes[4,20] have been identified as possible candidates for the electron traps. The presence of water has been linked to the formation of shallow hole traps, due to an energetic broadening of occupied states of the semiconductor in the presence of water molecules[21]. Similar effects have been reported for clusters of water[22]. To investigate whether water or oxygen itself could also be responsible for hole trapping, the IEs of these species were evaluated. The gas phase IE of water (12.65 eV)[23] or oxygen (12.06 eV)[24] are, however, much too high to cause hole trapping, even when considering stabilization by the dielectric medium. This implies isolated water or oxygen molecules in an organic semiconductor cannot function as hole traps.

This situation changes when clusters of water are considered. If a water molecule is surrounded by an H_2O shell, its IE can drastically decrease if dipole moments of the surrounding water coherently stabilize the charge on the water molecule. In fact, the very same mechanism is responsible for the difference in the optical and low-frequency relative permittivities of water (1.8 and 80). Statistically, there will always exist clusters with water orientations leading to potential traps.

To justify our proposition, we show that 'empty pockets' in organic materials are large enough to provide electrostatic stabilization capable of lowering the gas phase IE from 12 eV to 6 eV. To this end, we have evaluated the IEs of water clusters in amorphous morphologies of representative organic molecules, with a broad variation in IE and molecular packing. Molecular-dynamics simulations of amorphous films and perturbative calculations of IEs were performed as described in the Methods section. We note that these simulations represent a more realistic situation than the system of a single organic molecule surrounded by water[22], which does not include the stabilization effect of the surrounding organic molecules. A part of the simulated morphology for amorphous C_{60} is shown in Fig. 3. It is clear that 20–40 water molecules can fit inside the voids. For the other materials, the distributions of cluster sizes are shown in Supplementary Fig. 15.

Figure 4 shows the corresponding densities of states of organic materials and water clusters. The IE of a water cluster can be lower than the IE of C_{60} (6.4 eV), implying that clusters can act as hole traps. This agrees with the experimentally observed trap-limited hole transport in C_{60} and its energy position outside of the trap-free window. For CBP, with its IE (6.0 eV) at the border of the trap-free window, some clusters would still act as hole traps according to the simulations, which is also observed experimentally. Due to the low experimental hole-trap density of $7\times10^{15}\,cm^{-3}$ (Supplementary Fig. 2), hole transport in thin layers of CBP appears to be trap free, while thick layers reveal minor hole trapping. For NPB and TCTA, which have lower IEs of 5.4 eV and 5.7 eV, located inside the trap-free

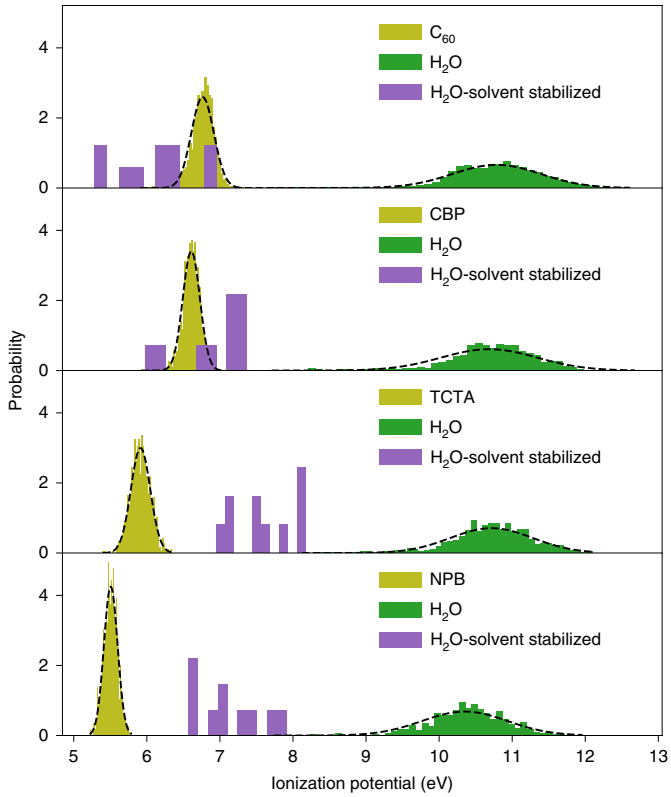

Fig. 4 | Calculated densities of states of water clusters in four organic films. The dark yellow distributions are the calculated density-of-states distributions of the organic semiconductors. Broad green distributions are clusters with random orientations of water molecules, violet peaks correspond to a few clusters were the water shell leads to a large dielectric screening of the charge. The larger the cluster, the stronger the stabilization.

window, hole trapping by water clusters would not be expected based on the simulations. This agrees with the experimental observation of trap-free hole transport in these materials.

A water-induced shift in energy of the occupied states of the organic semiconductor leading to shallow traps, as proposed recently[22], was not observed. This is because stabilization already occurs due to the surrounding organic molecules. Therefore, we would not expect water-related trapping inside the trap-free window. The absence of trapping is confirmed experimentally by the thickness- and time–dependence of the transport[5,8–16] (Supplementary Fig. 12). Since the devices were fabricated and characterized in an inert atmosphere the traps observed outside the trap-free window are already present in the material after synthesis or deposition and are not necessarily related to ambient exposure[25]. We have carried out ambient-exposure experiments, which show only minor but consistent effects on the device currents. However, the interpretation of these results is non-trivial, since it is not clear how much water is actually absorbed on air exposure and how this would translate in the number of additional traps, as discussed in more detail in Supplementary Section 6. We additionally demonstrate that hole traps in PCBM can be partially removed by thermal annealing, while transport in the trap-free ICBA control device was unaffected (Supplementary Fig. 14).

In conclusion, we have identified an energy window inside which organic semiconductors exhibit trap-free charge transport, applying to both small-molecule and polymeric organic semiconductors. In addition to the frequently observed electron trapping in organic semiconductors with an EA below 3.6 eV, it was found that hole trapping also occurs in materials with an IE beyond 6 eV, even in vacuum-deposited films of small molecules. Theoretical calculations reconcile this behaviour with water clusters acting as hole traps. This study on a large number of materials with a large variation in chemical structures shows that labelling organic semiconductors as being n-type, p-type or bipolar is directly related to the position of their energy levels with respect to the trap-free window. Balanced charge transport in devices such as organic solar cells and light-emitting diodes (OLEDs) requires the energy levels of the organic semiconductors to be situated within this energy window of around 2.4 eV, which is a design rule for efficient organic devices.

Online content

Any methods, additional references, Nature Research reporting summaries, source data, statements of code and data availability and associated accession codes are available at https://doi.org/10.1038/s41563-019-0473-6.

Received: 14 March 2019; Accepted: 31 July 2019;
Published online: 23 September 2019

References

1. Coropceanu, V. et al. Charge transport in organic semiconductors. *Chem. Rev.* **107**, 926–952 (2007).
2. Tang, M. L., Reichardt, A. D., Wei, P. & Bao, Z. Correlating carrier type with frontier molecular orbital energy levels in organic thin film transistors of functionalized acene derivatives. *J. Am. Chem. Soc.* **131**, 5264–5273 (**2009**).
3. Chua, L.-L. et al. General observation of N-type field-effect behaviour in organic semiconductors. *Nature* **434**, 194–199 (2005).
4. Nicolai, H. T. et al. Unification of trap-limited electron transport in semiconducting polymers. *Nat. Mater.* **11**, 882–887 (2012).
5. Kotadiya, N. B. et al. Universal strategy for ohmic hole injection into organic semiconductors with high ionization energies. *Nat. Mater.* **17**, 329–334 (2018).
6. Mott, S. N. F. & Gurney, R. W. *Electronic Processes in Ionic Crystals* 2nd edn (Clarendon Press, 1948).
7. Mark, P. & Helfrich, W. Space-charge-limited currents in organic crystals. *J. Appl. Phys.* **33**, 205–215 (1962).
8. Kotadiya, N. B., Blom, P. W. M. & Wetzelaer, G. A. H. Trap-free space-charge-limited hole transport in a fullerene derivative. *Phys. Rev. Appl.* **11**, 024069 (2019).
9. Wetzelaer, G.-J. A. H. et al. Asymmetric electron and hole transport in a high-mobility n-type conjugated polymer. *Phys. Rev. B* **86**, 165203 (2012).
10. Nicolai, H. T. et al. Space-charge-limited hole current in poly(9,9-dioctylfluorene) diodes. *Appl. Phys. Lett.* **96**, 172107 (2010).
11. Wetzelaer, G. A. H. & Blom, P. W. M. Ohmic current in organic metal-insulator-metal diodes revisited. *Phys. Rev. B* **89**, 241201 (2014).
12. Blom, P. W. M., de Jong, M. J. M. & Vleggaar, J. J. M. Electron and hole transport in poly(p-phenylene vinylene) devices. *Appl. Phys. Lett.* **68**, 3308–3310 (1996).
13. Rohloff, R., Kotadiya, N. B., Crăciun, N. I., Blom, P. W. M. & Wetzelaer, G. A. H. Electron and hole transport in the organic small molecule α-NPD. *Appl. Phys. Lett.* **110**, 073301 (**2017**).
14. Kotadiya, N. B. et al. Rigorous characterization and predictive modeling of hole transport in amorphous organic semiconductors. *Adv. Electron. Mater.* **4**, 1800366 (**2018**).
15. Karki, A. et al. Unifying energetic disorder from charge transport and band bending in organic semiconductors. *Adv. Funct. Mater.* **29**, 1901109 (2019).
16. Vissenberg, M. C. J. M. & Blom, P. W. M. Transient hole transport in poly(-p-phenylene vinylene) LEDs. *Synth. Met.* **102**, 1053–1054 (1999).
17. Torabi, S. et al. Strategy for enhancing the dielectric constant of organic semiconductors without sacrificing charge carrier mobility and solubility. *Adv. Funct. Mater.* **25**, 150–157 (2015).
18. Seemann, A. et al. Reversible and irreversible degradation of organic solar cell performance by oxygen. *Solar Energy* **85**, 1238–1249 (2011).
19. Nayak, P. K., Rosenberg, R., Barnea-Nehoshtan, L. & Cahen, D. O_2 and organic semiconductors: electronic effects. *Org. Electron.* **14**, 966–972 (2013).
20. Zhuo, J.-M. et al. Direct spectroscopic evidence for a photodoping mechanism in polythiophene and poly(bithiophene-alt-thienothiophene) organic semiconductor thin films involving oxygen and sorbed moisture. *Adv. Mater.* **21**, 4747–4752 (2009).
21. Nikolka, M. et al. High operational and environmental stability of high-mobility conjugated polymer field-effect transistors through the use of molecular additives. *Nat. Mater.* **16**, 356–362 (2017).
22. Zuo, G., Linares, M., Upreti, T. & Kemerink, M. General rule for the energy of water-induced traps in organic semiconductors. *Nat. Mater.* **18**, 588–593 (2019).

23. Page, R. H., Larkin, R. J., Shen, Y. R. & Lee, Y. T. High-resolution photoionization spectrum of water molecules in a supersonic beam. *J. Chem. Phys.* **88**, 2249–2263 (1988).
24. Tonkyn, R. G., Winniczek, J. W. & White, M. G. Rotationally resolved photoionization of O_2+ near threshold. *Chem. Phys. Lett.* **164**, 137–142 (1989).
25. de Leeuw, D. M., Simenon, M. M. J., Brown, A. R. & Einerhand, R. E. F. Stability of n-type doped conducting polymers and consequences for polymeric microelectronic devices. *Synth. Met.* **87**, 53–59 (1997).
26. Tanase, C., Meijer, E. J., Blom, P. W. M. & de Leeuw, D. M. Unification of the hole transport in polymeric field-effect transistors and light-emitting diodes. *Phys. Rev. Lett.* **91**, 216601 (2003).

Acknowledgements

The authors thank C. Bauer, M. Beuchel, Hs-J. Guttmann, F. Keller and V. Maus for technical support and Y. Ie for the synthesis of 4CzIPN. This project has received funding from the European Union Horizon 2020 research and innovation programme under grant agreement no. 646176 (EXTMOS) and no. 646259 (MOSTOPHOS). D.A. thanks the BMBF grant InterPhase (grant no. FKZ 13N13661).

Author contributions

G.A.H.W. proposed the project. N.B.K. carried out sample preparation and electrical measurements. G.A.H.W. and N.B.K. analysed the experimental data. A.M. and D.A. devised and performed molecular-dynamics simulations. G.A.H.W., P.W.M.B. and D.A. supervised the project and wrote the manuscript, with input from N.B.K. and A.M.

Competing interests

The authors declare no competing interests.

Additional information

Supplementary information is available for this paper at https://doi.org/10.1038/s41563-019-0473-6.

Reprints and permissions information is available at www.nature.com/reprints.

Correspondence and requests for materials should be addressed to G.-J.A.H.W.

Publisher's note: Springer Nature remains neutral with regard to jurisdictional claims in published maps and institutional affiliations.

Methods

Materials. 1,2,3,5-tetrakis(carbazol-9-yl)-4,6-dicyanobenzene (4CzIPN) was synthesized according to procedures described in the literature[27] and purified by vacuum sublimation. 4,4′′-bis(triphenylsilanyl)-(1,1′,4′,1′′)-terphenyl (BST) and 4,6-bis(3,5-di(pyridin-3-yl)phenyl)-2-(pyridin-3-yl)pyrimidine (B3PyPPM) were purchased from Luminescence Technology Corp. and all other materials were purchased from Sigma-Aldrich and used as received. All materials are listed in the Supplementary Information.

Device fabrication and characterization. Hole-only devices were generally fabricated in a glass/ITO/PEDOT:PSS(40 nm)/organic semiconductor/interlayer/MoO_3(10 nm)/Al(100 nm) structure, using a 3–5 nm interlayer with a higher IE than the main organic semiconductor, where ITO denotes indium-tin oxide and PEDOT:PSS denotes poly(3,4-ethylenedioxythiophene)-poly(styrenesulfonate). Electron-only devices were generally fabricated in a glass/Al(35 nm)/organic semiconductor/[TPBi(5 nm)]/Ba(5 nm)/Al(100 nm) structure, where TPBi denotes 1,3,5-tris(*N*-phenylbenzimidazol-2-yl)benzene. PEDOT:PSS was deposited by spin coating and organic layers were either thermally evaporated at a base pressure of $4–5\times10^{-7}$ mbar, or spin coated from chloroform solution (fullerene derivatives) under a nitrogen atmosphere. Electrical characterization was performed in a nitrogen-filled glovebox ($O_2<0.1$ ppm, $H_2O<0.1$ ppm) with a Keithley 2400 source meter. Devices were not exposed from organic semiconductor deposition until after the electrical measurements.

Computer simulations. To investigate the potential ability of water molecules acting as energy (hole) traps in organic semiconducting materials, atomistic molecular-dynamics simulations were first performed to acquire amorphous morphologies. Next, these morphologies were used to study the energy levels of different constituents by employing quantum chemical calculations and polarizable force fields. In the process of morphology simulations, the optimized potentials for liquid simulations, all-atom version (OPLS-AA)[28–31] force field was adapted for organic semiconductors such as C_{60}, NPB, TCTA and CBP[14]. To reparametrize the missing bonded interactions, density functional theory based calculations (at B3LYP/6-311+G(d,p) level of theory) were performed to scan the cross-sections of the potential energy surfaces, following the procedure described elsewhere[32,33]. The ChelpG scheme[34] was used to compute the atomic site charges. All Lennard-Jones parameters were taken from the OPLS force field[28–31], including the combination rules and a fudge-factor for 1–4 interactions of 0.5. On the other hand, extended simple point charge model (SPC/E) parameters[35] were used to model the water molecule. To obtain amorphous morphologies for studying energy traps for holes, 1,000 H_2O molecules were inserted into a pre-equilibrated simulation cell at 500 K of 3,000 molecules (except for C_{60}, 3,136 molecules) of organic semiconductors. Out of 1,000 molecules, ten molecules were considered to be an H_2O cation, resulting in a total charge of the system to be +10e. Atomic partial charges for the H_2O cation were computed via the ChelpG scheme[34]. The presence of H_2O cations results in a subtle imbalance in local charge distribution and consequently, surrounding neutral H_2O molecules orient their dipoles to stabilize the positively charged H_2O. Thus, the H_2O cations facilitate the formation of H_2O clusters which in turn can act as traps for holes in these organic molecules. In the next step, the system was annealed from 500 K to 800 K, which is above the glass transition temperature of organic molecules, followed by a very fast quenching to 300 K. Finally, equilibration of 2 ns duration followed by 1 ns production runs were performed at 300 K. A smooth particle mesh was employed. The Ewald technique was used to compute long-range electrostatic interactions. Non-bonded interactions were calculated in real-space using a cutoff of 1.3 nm. All calculations were performed in the NPT ensemble using a canonical velocity-rescaling thermostat[36] and the Berendsen barostat[37] as implemented in the GROMACS simulation package[38,39]. We utilized these molecular-dynamics trajectories to evaluate hole site energies by employing a perturbative method. In this approach, electrostatic and induction energies are added to the gas phase (IE_0) to obtain the total site energy[40–43]. For organic semiconductors (except for C_{60}, experimentally measured values were used), adiabatic IE_0 values were computed at the M062X/6-311+g(d,p) level of theory using the Gaussian09 programme[44]. For H_2O, gas phase ion energies were obtained from the NIST database[23]. The electrostatic and induction contribution to the site energies were calculated self-consistently using the Thole model[45,46] on the basis of the atomic polarizabilities and distributed multipoles, obtained by using the GDMA programme[47] for a neutral, cation and an anion molecule. Calculations were performed using the VOTCA-CTP package[48].

Data availability

Experimental data are available from the corresponding author upon reasonable request.

References

27. Uoyama, H., Goushi, K., Shizu, K., Nomura, H. & Adachi, C. Highly efficient organic light-emitting diodes from delayed fluorescence. *Nature* **492**, 234–238 (2012).
28. Jorgensen, W. L. & Tirado-Rives, J. The OPLS [optimized potentials for liquid simulations] potential functions for proteins, energy minimizations for crystals of cyclic peptides and crambin. *J. Am. Chem. Soc.* **110**, 1657–1666 (1988).
29. Jorgensen, W. L., Maxwell, D. S. & Tirado-Rives, J. Development and testing of the OPLS all-atom force field on conformational energetics and properties of organic liquids. *J. Am. Chem. Soc.* **118**, 11225–11236 (1996).
30. Jorgensen, W. L. & Tirado-Rives, J. Potential energy functions for atomic-level simulations of water and organic and biomolecular systems. *Proc. Natl Acad. Sci. USA* **102**, 6665–6670 (2005).
31. McDonald, N. A. & Jorgensen, W. L. Development of an all-atom force field for heterocycles. Properties of liquid pyrrole, furan, diazoles, and oxazoles. *J. Phys. Chem. B* **102**, 8049–8059 (1998).
32. Poelking, C. et al. Characterization of charge-carrier transport in semicrystalline polymers: electronic couplings, site energies, and charge-carrier dynamics in poly(bithiophene-*alt*-thienothiophene) [PBTTT]. *J. Phys. Chem. C* **117**, 1633–1640 (2013).
33. Poelking, C. & Andrienko, D. Effect of polymorphism, regioregularity and paracrystallinity on charge transport in poly(3-hexyl-thiophene) [P3HT] nanofibers. *Macromolecules* **46**, 8941–8956 (2013).
34. Breneman, C. M. & Wiberg, K. B. Determining atom-centered monopoles from molecular electrostatic potentials. The need for high sampling density in formamide conformational analysis. *J. Comput. Chem.* **11**, 361–373 (1990).
35. Berendsen, H. J. C., Grigera, J. R. & Straatsma, T. P. The missing term in effective pair potentials. *J. Phys. Chem.* **91**, 6269–6271 (1987).
36. Bussi, G., Donadio, D. & Parrinello, M. Canonical sampling through velocity rescaling. *J. Chem. Phys.* **126**, 014101 (2007).
37. Berendsen, H. J. C., Postma, J. P. M., Gunsteren, W. F., van; DiNola, A. & Haak, J. R. Molecular dynamics with coupling to an external bath. *J. Chem. Phys.* **81**, 3684–3690 (1984).
38. Pronk, S. et al. GROMACS 4.5: a high-throughput and highly parallel open source molecular simulation toolkit. *Bioinformatics* **29**, 845–854 (2013).
39. Van Der Spoel, D. et al. GROMACS: fast, flexible, and free. *J. Comput. Chem.* **26**, 1701–1718 (2005).
40. Poelking, C. & Andrienko, D. Long-range embedding of molecular ions and excitations in a polarizable molecular environment. *J. Chem. Theory Comput.* **12**, 4516–4523 (**2016**).
41. Poelking, C. & Andrienko, D. Design rules for organic donor-acceptor heterojunctions: pathway for charge splitting and detrapping. *J. Am. Chem. Soc.* **2015**, 6320–6326.
42. Poelking, C. et al. Impact of mesoscale order on open-circuit voltage in organic solar cells. *Nat. Mater.* **14**, 434–439 (2015).
43. D'Avino, G. et al. Electrostatic phenomena in organic semiconductors: fundamentals and implications for photovoltaics. *J. Phys.: Condens. Matter* **28**, 433002 (2016).
44. Frisch, M. J. et al. Gaussian 16 Revision B.01 (Gaussian, Inc., 2016).
45. Thole, B. T. Molecular polarizabilities calculated with a modified dipole interaction. *Chem. Phys.* **59**, 341–350 (1981).
46. Van Duijnen, P. Th & Swart, M. Molecular and atomic polarizabilities: Thole's model revisited. *J. Phys. Chem. A* **102**, 2399–2407 (1998).
47. Stone, A. J. Distributed multipole analysis—stability for large basis sets. *J. Chem. Theory Comput.* **1**, 1128–1132 (2005).
48. Ruehle, V. et al. Microscopic simulations of charge transport in disordered organic semiconductors. *J. Chem. Theory Comput.* **7**, 3335–3345 (2011).